

## Gene transfer of insulin-like growth factor–I providing neuroprotection after spinal cord injury in rats

KUO-SHENG HUNG, M.D., PH.D.,<sup>1</sup> SHIN-HAN TSAI, M.D., PH.D.,<sup>1</sup> TAO-CHEN LEE, M.D.,<sup>2</sup> JIA-WEI LIN, M.D.,<sup>1</sup> CHENG-KUEI CHANG, M.D., PH.D.,<sup>3</sup> AND WEN-TA CHIU, M.D., PH.D.<sup>1</sup>

<sup>1</sup>Department of Neurosurgery, Graduate Institute of Injury Prevention and Control, Taipei Medical University, Wan Fang Medical Center, Taipei; <sup>2</sup>Department of Neurosurgery, Chang Gung University College of Medicine, Chang Gung Medical Center, Kaohsiung County; <sup>3</sup>Department of Neurosurgery, Mackay Memorial Hospital and Graduate Institute of Injury Prevention and Control, Taipei Medical University, Taipei, Taiwan

**Object.** Insulin-like growth factor–I (IGF-I) has been shown to be a potent neurotrophic factor that promotes the growth of projection neurons, dendritic arborization, and synaptogenesis. Its neuroprotective roles may be coordinated by activation of Akt, inhibition of glycogen synthase kinase–3 $\beta$  (GSK-3 $\beta$ ), and thus inhibition of tau phosphorylation. The authors investigated the role and mechanism of IGF-I gene transfer after spinal cord injury (SCI).

**Methods.** Studies were performed in 40 male Sprague–Dawley rats after spinal cord hemisection. The authors conducted hydrodynamics-based gene transfection in which an IGF-I plasmid was rapidly injected into the rat's tail vein 30 minutes after SCI. The animals were randomly divided into four groups: Group I, sham operated; Group II, SCI treated with *pCMV-IGF-I* gene; Group III, SCI treated with vehicle *pCMV-LacZ* gene; and Group IV, SCI only. The results showed that IGF-I gene transfer promoted motor recovery, antiinflammatory responses, and anti-apoptotic effects after SCI. Using techniques of Western blotting and immunohistochemistry, the authors assessed the mechanism of IGF-I gene transfer after SCI in terms of activation of Akt, inhibition of GSK-3 $\beta$ , attenuation of p35, and inhibition of tau phosphorylation. Moreover, they found that IGF-I gene transfer could block caspase-9 cleavage, increase Bcl-2 formation, and thus inhibit apoptosis after SCI.

**Conclusions.** The intravenous administration of IGF-I after SCI activated Akt, attenuated GSK-3 $\beta$ , inhibited p35 activation, diminished tau hyperphosphorylation, ended microglia and astrocyte activation, inhibited neuron loss, and significantly improved neurological dysfunction. Furthermore, IGF-I attenuated caspase-9 cleavage, increased Bcl2, and thus inhibited apoptosis after SCI.

**KEY WORDS** • insulin-like growth factor–I • spinal cord injury • gene transfer • apoptosis

**S**PINAL cord injury is devastating for the individual and costly to society because it requires substantial long-term healthcare expenditures. Within minutes of primary injury, a cascade of biochemical events is initiated, leading to secondary cell death that evolves over a period of days to weeks. Various molecular pathways may be involved including hypoxia, ischemia, intracellular and extracellular ionic shifts, lipid peroxidation, free radical production, excitotoxicity, eicosanoid production, neutral protease activation, prostaglandin production, and programmed cell death or apoptosis. The result is that, days or weeks after SCI, some of the neuronal and glial

supporter cells die, even though they survived the initial injury.<sup>11</sup> Currently, high-dose methylprednisolone administered within 8 hours of injury is the only therapy with recognized benefit,<sup>3</sup> which, unfortunately, is relatively minor. We have demonstrated that p35–p25–Cdk5 activation, tau hyperphosphorylation, and apoptosis could be the reasons for neural damage after spinal cord hemisection.<sup>10</sup> Any new treatment of SCI that allows for major recovery of both functional and molecular levels would be a significant advance.

Insulin-like growth factor–I has been shown to be a potent neurotrophic factor that promotes the growth of projection neurons, dendritic arborization, and synaptogenesis.<sup>4,16</sup> Insulin-like growth factor–I acts in an autocrine and paracrine manner to promote glucose utilization, using phosphatidylinositol 3–kinase/Akt and the downstream GSK-3 $\beta$  pathways.<sup>5,9</sup> Its neuroprotective roles may be coordinated by activation of Akt, inhibition of GSK-3 $\beta$ , and thus inhibition of tau phosphorylation.<sup>5,9</sup> The role and mechanism of IGF-I gene transfer after SCI are, however, still unknown.

*Abbreviations used in this paper:* BBB = Basso-Beattie-Bresnahan; Cdk5 = cyclin-dependent kinase 5; ELISA = enzyme-linked immunosorbent assay; GFAP = glial fibrillary acidic protein; GSK-3 $\beta$  = glycogen synthase kinase–3 $\beta$ ; IGF-I = insulin-like growth factor–I; PBS = phosphate-buffered saline; SCI = spinal cord injury; SEM = standard error of the mean; TUNEL = terminal deoxynucleotidyl transferase-mediated deoxyuridine triphosphate nick-end labeling.

In the mouse model of amyotrophic lateral sclerosis, Kaspar et al.<sup>12</sup> recently showed that apoptosis of motor neurons was markedly attenuated by retrograde adenoviral delivery of IGF-I through the mechanism of upregulation of phospho-Akt and downregulation of caspase-9 cleavage. Furthermore, Pan and Kastin<sup>17</sup> demonstrated that systemically administered IGF-I enters the central nervous system via a saturable transport system at the blood-brain barrier, as predicted on consideration of the size, and effectively prevents cellular injury and inflammation when given after ischemic trauma. These findings suggest that IGF-I provides early recovery of neuronal function in cases of hypoxic ischemia and amyotrophic lateral sclerosis. These treatments, however, require multiple intravenous, intraperitoneal, or intramuscular administrations of IGF-I.

We have developed a strategy in which a plasmid vector containing the genes of interest is injected directly into a vein.<sup>21,22</sup> This approach represents a promising new strategy to deliver and express foreign genes *in vivo* and has obvious advantages including the easy preparation of a large amount of plasmids, continuous expression of targeted protein, and proven safety *in vivo*. In the present study, we describe a hydrodynamics-based transfection procedure utilizing intravenous administration of naked IGF-I plasmid that results in significant high levels of exogenous IGF-I protein expression in the spinal cord.

To delineate the nature and mechanism of the IGF-I gene therapy in SCI, we evaluated the effects of intravenous IGF-I plasmid infusion in rats with spinal cord hemisection. The specific aims were to answer the following questions. 1) Can intravenous administration of naked IGF-I plasmid transfect the spinal cord after cord hemisection? 2) Do alterations in motor function occur after IGF-I gene transfer? 3) What is the effect of the changes in neuron survival by IGF-I gene therapy on cord hemisection? 4) Can IGF-I gene transfer inhibit glial scarring and microglia activation after SCI? 5) Does activation of Akt, inhibition of GSK-3 $\beta$ , attenuation of p35, and inhibition of tau phosphorylation occur after IGF-I gene transfer? 6) Does cleavage of caspase-9, Bcl2, and apoptosis change in an IGF-I plasmid-treated group compared with those treated with control vectors? The overall objective of this study was to determine the neuroprotective, anti-inflammatory, and antiapoptotic effects of IGF-I gene transfer in SCI.

## Materials and Methods

### Animal Care

Male Sprague-Dawley rats (Academia Sinica), weighing 280 to 330 g, were kept two per cage for at least 5 days after their arrival at our laboratory. The rats had access to food and water *ad libitum* and were housed within a room with a 12:12 hour dark-light cycle. This study was performed in accordance with the guidelines provided by the Experimental Animal Laboratory and approved by the Animal Care and Use Committee at Wan Fang Medical Center.

### Induction of Spinal Cord Hemisection Injury in Rats

For hemisection, the rats received isoflurane inhalational anesthesia and were placed in a spinal cord unit of a stereotaxic apparatus (David Kopf Instruments). Using an adjustable wire knife, we made a lesion on the left side of the rats' spinal cords (30 rats) or

performed a sham operation (10 rats). Laminectomy was performed at T-11 with delicate diamond drills, and the wire knife guide was placed in a vertical plane close to the lateral surface of the lower thoracic level of the spinal cord. This level was chosen so that cranial and caudal nonlesioned segments of the spinal cord could be analyzed. The knife, which was previously turned medially, was then extended 1.5 mm and the guide was lifted 4.0 mm to hemisection the spinal cord. Iridectomy scissors were used to ensure the completeness of the hemisection.<sup>10</sup> The fascia and skin were closed with sutures by layer, and the animals were allowed to recover while lying on a 36.5°C heating pad. Following surgery, animals were maintained under the same preoperative conditions and were eating and drinking within 3 hours of surgery. Weight loss was minimal, occurred acutely over the first 2 postoperative days, and did not exceed 5% of the total body weight. The extent of the hemisection lesion, assessed histologically, was confined unilaterally and included the dorsal column, Lissauer tract (dorsolateral fasciculus), lateral and ventral column systems, and gray matter. Locomotor function was measured using the BBB Locomotor Rating Scale<sup>2</sup> to ensure that a motor deficit of the ipsilateral limb had occurred. The animals exhibiting loss of locomotion in both hindlimbs were excluded from the study. The sham operation consisted of laminectomy without spinal cord hemisection.

### Animal Grouping, Plasmid Injection, and IGF-I Expression

The full-length of human IGF-I cDNA was subcloned into pCMV-MCS vector (Stratagene) to create the human IGF-I expression plasmid (pCMV-IGF-I). The pCMV-LacZ plasmid was used as a vehicle control. The plasmids were purified using the EndoFree Plasmid Giga Kit (Qiagen). Forty male Sprague-Dawley rats were randomly divided into four groups: Group I, treated with sham surgery; Group II, underwent SCI and treated with pCMV-IGF-I gene; Group III, underwent SCI and treated with vehicle pCMV-LacZ gene; and Group IV, underwent SCI only. Plasmids of pCMV-IGF-I and pCMV-LacZ were, respectively, injected into IGF-I-treated and vehicle-treated groups. The plasmid DNA was administered *in vivo* to rats using a hydrodynamics-based gene transfer technique that involved rapid injection of a large volume of DNA solution through the tail vein 30 minutes after cord hemisection.<sup>21,22</sup> Briefly, a certain amount of plasmid DNA (3  $\mu$ g/g) was diluted in 15 ml of saline and injected via the tail vein into the circulation within 15 seconds.

For analysis of IGF-I peptide expression, we obtained blood samples from cardiac puncture site after induction of isoflurane anesthesia 1, 7, and 14 days after the gene transfer procedure. The amount of plasma IGF-I was measured using an ELISA method, with minimum detectable concentration of 0.15 ng/ml, according to the user's manual (R&D Systems).

### Histological Features, Immunohistochemical Findings, and Cell Count

On the 14th day after hemisection-induced SCI, several rats (five in each group) were deeply anesthetized with isoflurane and received a left-ventricle perfusion of PBS, followed by cold 4% paraformaldehyde in 0.15 M sodium phosphate buffer, pH 7.4. The spinal cord was removed immediately, postfixed for 8 hours in the same fixative at 4°C, and cryoprotected for 2 to 3 days in 15 and 30% sucrose. The spinal cord was frozen in powdered dry ice and stored at -280°C until needed. Five-micrometer sections of the spinal cord hemisection were cut with a freezing and sliding microtome at the center. The sections were prepared for either immunostaining or apoptosis staining. For immunohistochemistry, sections were washed in PBS and incubated in 3% normal goat serum with 0.3% Triton X-100 in PBS for 1 hour. The sections were incubated free floating at 4°C with anti-IGF-I (1:100, Santa Cruz Biotechnology, Inc.), anti-NeuN (1:500, Chemicon), anti-GFAP (1:500, Dako-Cytomation), anti-CD11b (OX-42; 1:100, Chemicon), anti-p35 (C-19; 1:500, Santa Cruz), or anti-phospho-tau (AT8) (1:50, Pierce Biotechnology) antibodies. Immunoreactivity was visualized using the Vectastain Elite ABC Peroxidase method (Vector Laboratories) and diaminobenzidine as the chromagen. Furthermore, apoptosis after hemisection was detected by TUNEL in which we used an apoptosis detection kit (Oncogene Research Products). Terminal deoxy-

## Insulin-like growth factor-I gene transfer in SCI

nucleotidyl transferase-mediated deoxyuridine triphosphate nick-end labeling was performed according to the manufacturer's instructions. A negative control of TUNEL staining was generated by omission of Klenow enzyme, whereas the negative control sections of other immunohistochemical studies were incubated without primary antibodies. Cell counting was performed on every sixth section at the center of spinal cord hemisection stained with the aforementioned antibodies at a magnification of 400. Only cells with clearly visible staining were counted. All data are presented as means  $\pm$  SEMs of five consecutive cell quantifications.

### Immunoblot Analysis

For immunoblotting, spinal cord samples (five in each group) were homogenized in ice-cold modified radioimmunoprecipitation buffer (50mM Tris-HCl, pH 7.4, 150 mM NaCl, 1 mM ethylenediaminetetraacetic acid, 1 mM phenylmethylsulfonyl fluoride, 1% NP-40, 0.25% Na-deoxycholate, 1 mM  $\text{Na}_2\text{VO}_4$ , 1 mM NaF, 1  $\mu\text{g/ml}$  each of aprotinin, pepstatin, and leupeptin). Lysates were clarified by centrifugation for 15 minutes at 4°C. Protein concentrations were determined using the BCA protein assay (Pierce Biotechnology, Inc.). Twenty-five-microgram protein extracts were electrophoresed on a 10 or 12% acrylamide sodium dodecyl sulfate-polyacrylamide gel electrophoresis and immunoblotted onto polyvinylidene fluoride membranes. The membranes were blocked for 1 hour in TBST (10 mM Tris-HCl pH 7.6, 150 mM NaCl, 0.1% Tween-20) containing 5% weight/volume nonfat dry milk and then incubated overnight with the various primary antibodies. The antibodies used were anti-phospho-Akt (Ser-473; 1:1000, Cell Signaling Technology, Inc.), anti-Akt (1:1000, Cell Signaling), anti-phospho-GSK-3 $\beta$  (Ser9; 1:1000, Cell Signaling), anti-GSK-3 $\beta$  (1:1000, Cell Signaling), anti-caspase-9 (1:1000, Cell Signaling), Anti-Bcl2 (1:1000, R&D Systems, Inc.), anti-Cdk5 (1:1000, Santa Cruz Biotechnology), and anti- $\beta$ -actin (1:5000, Sigma-Aldrich Biotechnology, Inc.). Immunoreactivity was demonstrated with horseradish peroxidase-conjugated goat anti-rabbit or anti-mouse (1:5000; Jackson ImmunoResearch Laboratories, Inc.) and the SuperSignal West Pico Chemiluminescent Substrate (Pierce). The band intensities were quantified by using the Fluor-S Multimager (Bio-Rad Laboratories, Inc.).

### Statistical Analysis

All data are presented as means  $\pm$  SEMs (with the means derived from a minimum of three experiments). Statistical analysis was performed using a one-way analysis of variance. A probability value less than 0.05 was considered significant.

## Results

### Expression of IGF-I In Vivo by a Single Administration of Naked Plasmid

To deliver exogenous IGF-I gene efficiently, we developed an in vivo gene transfection procedure in which a large volume of naked plasmid DNA solution is rapidly injected into the tail vein.<sup>21,22</sup> The presence of IGF-I in serum was analyzed with an ELISA kit. As shown in Fig 1, a single intravenous administration of the pCMV-IGF-I plasmid resulted in marked IGF-I expression. We used a certain amount of plasmid DNA (3  $\mu\text{g/g}$ ) diluted in 15 ml of saline and injected the plasmid via the tail vein into the circulation within 15 seconds. The levels of IGF-I protein in the circulation could reach as high as 80 ng/ml 1 day following intravenous injection (Fig. 1). Although the circulating level of IGF-I began to decline thereafter, a significant amount of IGF-I protein was still found in the circulation 14 days after the initial injection of pCMV-IGF-I plasmid compared with that observed in the pCMV-LacZ

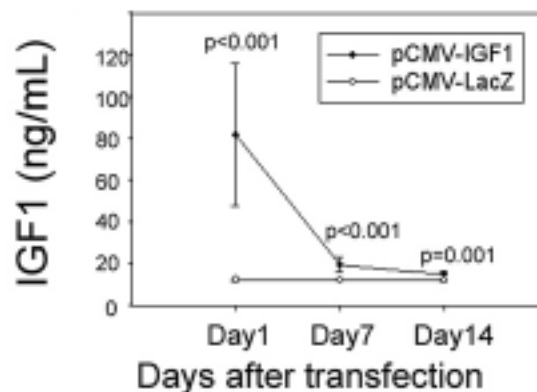


FIG. 1. Graph showing the distribution of IGF-I levels following a single injection of naked pCMV-IGF-I or pCMV-LacZ plasmid. At different time points as indicated, the plasma was collected, and the IGF-I levels were determined by a specific ELISA for IGF-I protein. Significantly higher levels of IGF-I were noted in IGF-I groups than in the LacZ Group 1, 7, and 14 days after administration (pCMV-IGF-I compared with pCMV-LacZ [ $p < 0.001$  on Days 1 and 7;  $p = 0.001$  on Day 14]). Data are presented as means  $\pm$  SEMs (10 rats in each group).

group (pCMV-IGF-I compared with pCMV-LacZ: Day 1  $p < 0.001$ , Day 7  $p < 0.001$ , and Day 14  $p = 0.001$ ).

### Expression of IGF-I in the Spinal Cord 14 Days After Gene Transfer

We further checked the IGF-I expression in the spinal cords immunohistochemically 14 days after intravenous administration of naked IGF-I plasmid (Fig. 2). Insulin-like growth factor-I was markedly expressed at the spinal cord hemisection in the pCMV-IGF-I group but not in the negative control group (Fig. 2B). There was scant staining in the sham (Fig. 2A), pCMV-LacZ (Fig. 2C), and SCI (Fig. 2D) groups. In our model, IGF-I gene therapy could directly transfect the injured spinal cord.

### Effects of IGF-I Gene Transfer on Motor Function and Neuron Survival After Hemisection

To evaluate the presence and extent of neurological impairment after SCI, we used the BBB locomotor scales. The BBB scores of the affected hindlimbs significantly improved in the pCMV-IGF-I group compared with those in the pCMV-LacZ (vehicle) and SCI groups 7 and 14 days after SCI (on Days 7 and 14: pCMV-IGF-I compared with pCMV-LacZ  $p < 0.001$ ; pCMV-IGF-I compared with SCI  $p < 0.001$ ) (Fig. 3). Immunohistochemical assessment of NeuN, a neuron-specific marker, disclosed severe neuron loss in the vehicle and SCI groups 14 days after hemisection (sham compared with SCI  $p < 0.001$ ; sham compared with pCMV-LacZ  $p < 0.001$ ) (Fig. 4). Significant preservation of neurons was noted in the pCMV-IGF-I group (pCMV-IGF-I compared with SCI  $p < 0.001$ ; pCMV-IGF-I compared with pCMV-LacZ  $p < 0.001$ ) (Fig. 4). Evaluation of these data suggested that IGF-I gene therapy can prevent neurological deficits and neuronal loss after spinal cord hemisection and thus provided the reason why the BBB motor scores improved.

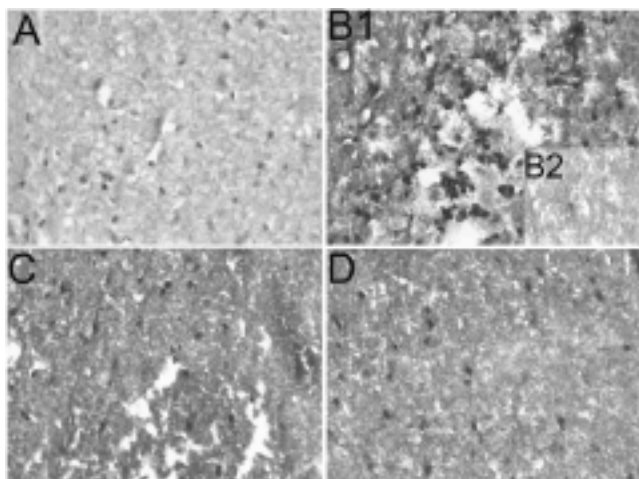


FIG. 2. Representative photomicrographs of IGF-I-stained spinal cord sections obtained in rats. A: There was scant staining in sham, LacZ, and SCI groups. B1: Marked staining for IGF-I was detected in the injured cord 14 days following gene transfer in the IGF-I group. B2: There was no staining for IGF-I in negative controls (omission of the first antibody). C: The LacZ group. D: The SCI group. Original magnification  $\times 400$ .

#### Effects of IGF-I Gene Therapy on Astrocyte and Microglia Activation After SCI

Astrocyte and microglia activation are the major inflammatory responses after SCI.<sup>10</sup> The expression of GFAP and CD11b, a marker of activated astrocytes and microglia, was investigated. Strong immunostaining of GFAP and CD11b was demonstrated in the spinal cord lesion, but these activations were greatly attenuated in the pCMV-IGF-I group (Fig. 5). These results showed that IGF-I gene transfer attenuates activation of astrocytes and microglia after SCI.

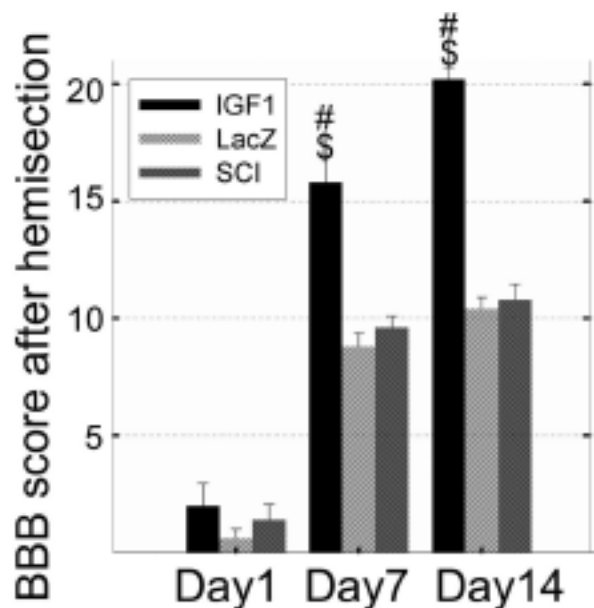


FIG. 3. Bar graph showing that IGF-I gene transfer, compared with vehicle, improves BBB scores of the affected hindlimbs 7 and 14 days after SCI. A normal limb would receive a score of 21 on the BBB scale. Scores significantly improved in pCMV-IGF-I group compared with the pCMV-LacZ (vehicle) and SCI groups 7 and 14 days after SCI (pCMV-IGF-I compared with pCMV-LacZ <sup>#</sup> $p < 0.001$ ; pCMV-IGF-I compared with SCI <sup>\$</sup> $p < 0.001$  on Days 7 and 14 [10 animals in each group]).

#### Insulin-Like Growth Factor-I Gene Transfer Activates Akt, Inhibits GSK-3 $\beta$ , and Attenuates p35 Activation and Tau Phosphorylation

To investigate the mechanism of IGF-I gene therapy after SCI, we first used immunohistochemistry and

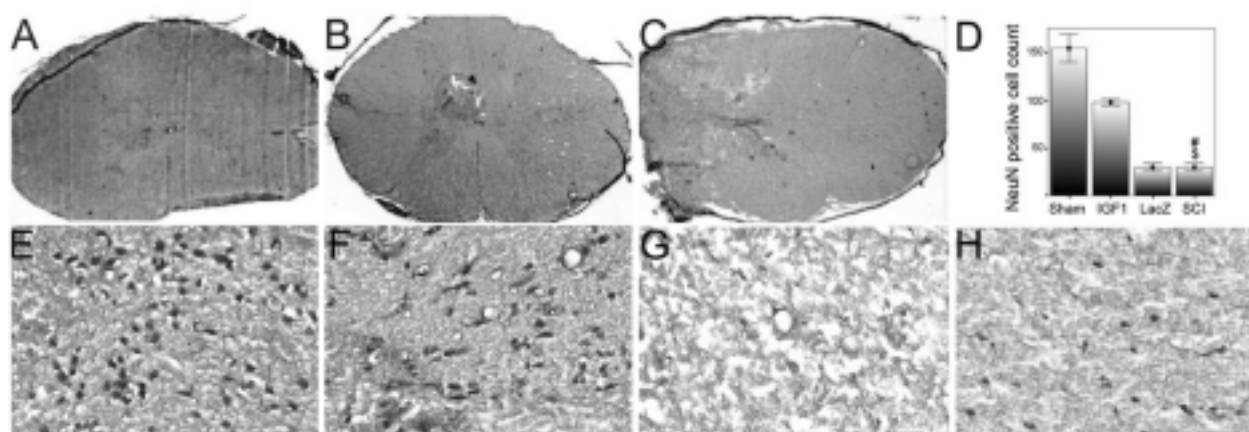


FIG. 4. Representative photomicrographs (A-C and E-H) of NeuN-stained sections of the spinal cords acquired in sham controls (A and E), hemisection with IGF-I gene transfer (B and F), hemisection with LacZ vehicle treatment (C and G), and hemisection (SCI) without treatment (H). Note that there are normal neurons in the sham group (E) and relative preservation of NeuN-stained neurons in the IGF-I group (F) compared with severe neuron loss in the vehicle (G) and SCI (H) groups. Original magnifications  $\times 12$  (A-C) and  $\times 400$  (E-H). D: Bar graph plotting results of the histopathological findings. Vertical bars indicate the mean ( $\pm$  SEM) number of neurons per tissue section for the sham controls (sham), hemisection with IGF-I gene transfer (IGF-I), hemisection with LacZ vehicle treatment (LacZ), and hemisection without treatment (SCI) (<sup>#</sup> $p < 0.001$ , sham compared with SCI;  $p < 0.001$ , sham compared with LacZ; <sup>\$</sup> $p < 0.001$  IGF-I compared with SCI;  $p < 0.001$ , IGF-I compared with LacZ [five animals in each group]).

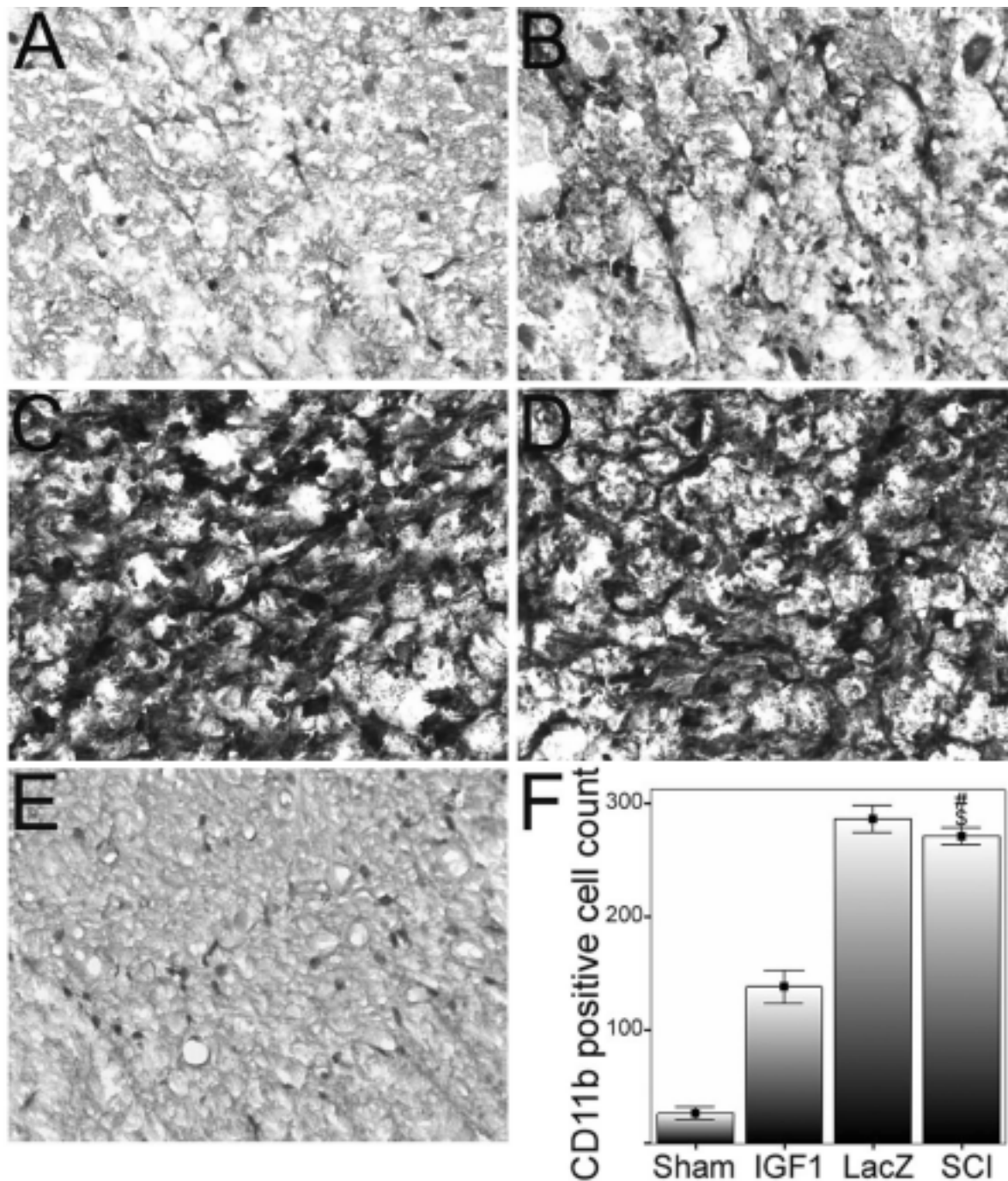


FIG. 5. A–E: Representative photomicrographs of CD11b-stained sections of the spinal cords obtained in the sham control (A), IGF-I (B), LacZ (C), SCI (D), and negative control (omission of primary antibody) of LacZ (E) groups 14 days after hemisection. Strong staining of CD11b-positive cells was demonstrated in the spinal cord lesion (C and D), whereas IGF-I gene administration markedly attenuated this upregulation (B). Original magnification  $\times 400$ . F: Bar graph plotting results of histopathological findings. Vertical bars indicate the mean ( $\pm$  SEM) number of CD11b-stained cells per tissue section for the sham control (sham), hemisection with IGF-I gene transfer (IGF-I), hemisection with LacZ vehicle treatment (LacZ), and hemisection without treatment (SCI) groups (\* $p < 0.001$ , sham compared with SCI;  $p < 0.001$ , sham compared with LacZ;  $^{\$}p < 0.001$ , IGF-I compared with SCI;  $^{\#}p < 0.001$ , IGF-I compared with LacZ [five animals in each group]).

Western blotting to test the phosphorylated Akt at Ser473. Upregulation of phosphorylated Akt was shown in the pCMV-IGF-I group 14 days after hemisection by both

immunohistochemistry (Fig. 6A–E) and Western blot analysis (Fig. 6F). Additionally, an increasing ratio of inhibitory phosphorylation of GSK-3 $\beta$  at Ser9/GSK-3 $\beta$

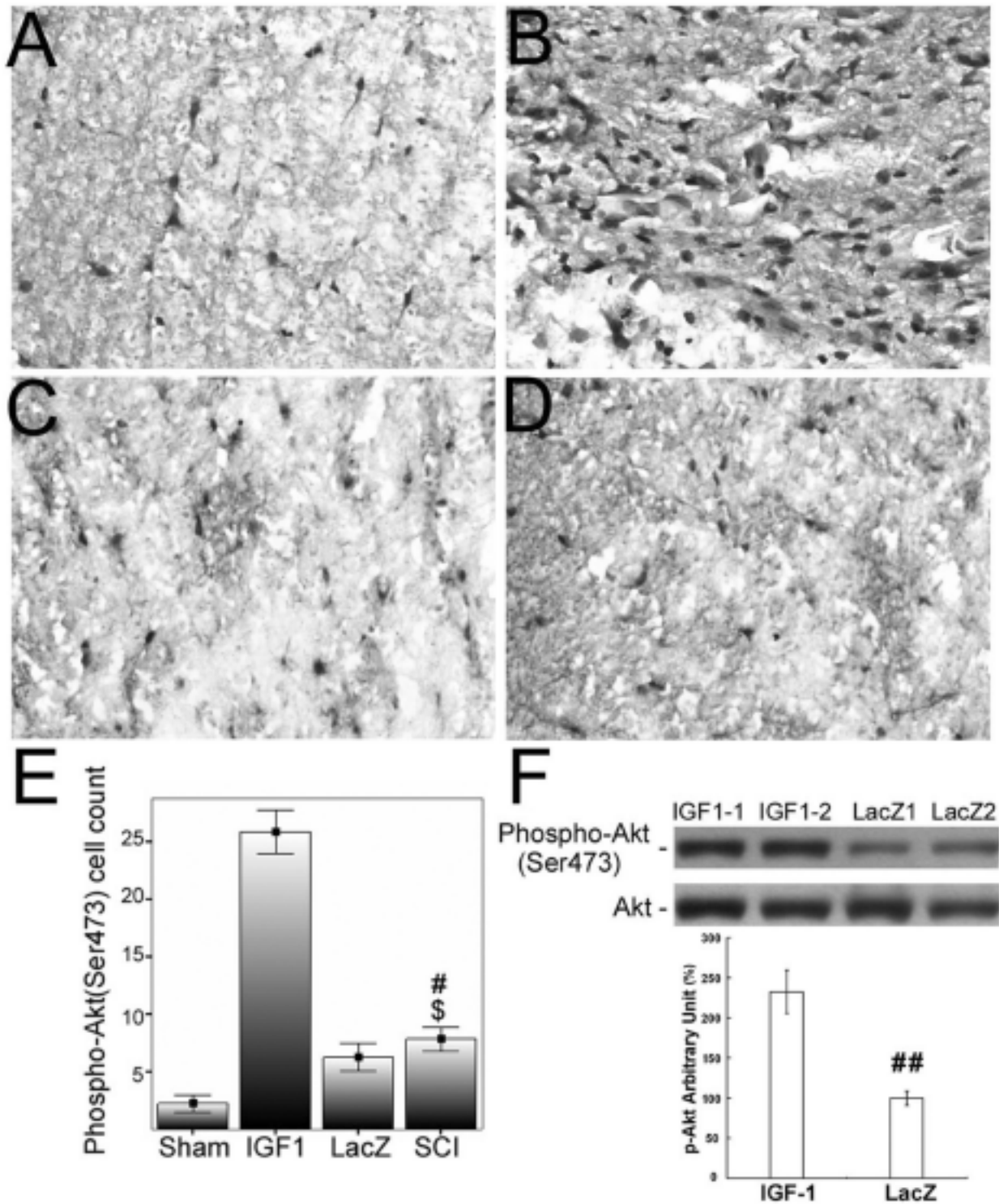


FIG. 6. A–D: Representative immunostained sections of phosphorylated Akt in sham control (A), IGF-I group (B), LacZ group (C), SCI group (D) and Western blotting (F)—all obtained 14 days after hemisection. Upregulation of phosphorylated Akt was noted in the IGF-I group compared with other groups. E: Graph. Vertical bars indicate the mean ( $\pm$  SEM) number of phosphorylated Akt-stained cells per tissue section for the sham controls (sham), hemisection with IGF-I gene transfer (IGF-I), hemisection with LacZ vehicle treatment (LacZ), and hemisection without treatment (SCI) ( $^{\#}p = 0.018$ , sham compared with SCI;  $^{\$}p < 0.001$ , IGF-I compared with SCI;  $p < 0.001$ , IGF-I compared with LacZ;  $p < 0.001$ , IGF-I compared with sham [five animals in each group]). F: Western blot analysis confirming the upregulation of phosphorylated Akt/Akt in the IGF-I group compared with the LacZ group ( $^{\#\#}p < 0.01$ , in arbitrary units, IGF-I compared with LacZ [five animals in each group]).

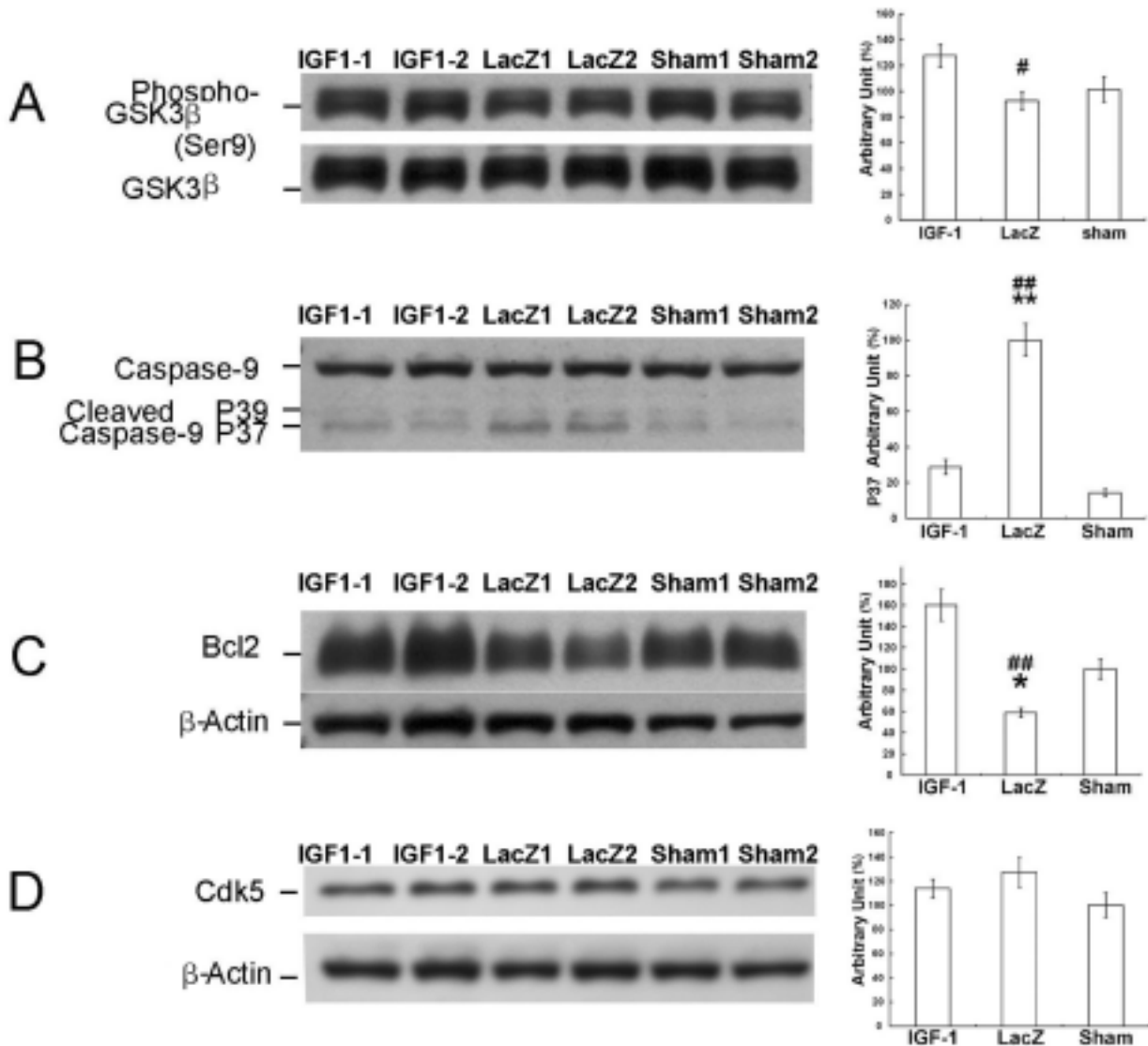


Fig. 7. Representative panels and graphs showing inhibitory phosphorylation of GSK-3 $\beta$  at Ser9 (A), caspase-9 (B), Bcl2 (C), and Cdk5 (D) expressions in spinal cord by immunoblotting 14 days after hemisection. Upregulation of inhibitory phosphorylation of GSK-3 $\beta$  and Bcl2 expression was noted in the IGF-I group compared with the LacZ group (phospho-GSK-3 $\beta$ ; IGF-I compared with LacZ [ $*p < 0.05$ ]) (Bcl2; IGF-I compared with LacZ [ $p < 0.01$ ]; sham vs. LacZ [ $*p < 0.05$ ]). Downregulation of cleaved caspase-9 expression (P37 and P39) was noted 14 days after IGF-I gene transfer (IGF-I compared with LacZ [ $##p < 0.01$ ]; sham compared with LacZ [ $**p < 0.01$ ]). However, there was no significant difference in Cdk5 expression. Arbitrary unit was defined as phosphor-GSK-3 $\beta$ /GSK-3 $\beta$  (A), P37/caspase-9 (B), Bcl2/ $\beta$ -actin (C), Cdk5/ $\beta$ -actin (D). There were five animals in each group.

was noted in the pCMV-IGF-I group compared with the pCMV-LacZ group (Fig. 7A). In a recent study we have revealed p35-p25-Cdk5 activation and tau hyperphosphorylation in the pathogenesis of SCI.<sup>10</sup> In the present study, we further demonstrated that IGF-I gene therapy could also significantly attenuate p35 activation (Fig. 8) and tau phosphorylation (Fig. 9) without significantly interfering in Cdk5 protein levels (Fig. 7D). Therefore, we have confirmed that the mechanisms of IGF-I gene transfer in SCI include activation of phosphorylated Akt, inhibition of GSK-3 $\beta$ , inactivation of p35, and attenuation of phosphorylated tau.

*Insulin-Like Growth Factor-I Gene Transfer Inhibits Cleavage of Caspase-9, Increases Bcl2 Expression, and Attenuates Apoptosis*

To investigate signaling within the apoptotic pathway, we tested the cleavage of caspase-9 and Bcl2 expression by immunoblotting. Insulin-like growth factor-I gene therapy was able to markedly reduce the amount of caspase-9 cleavage (Fig. 7B) and increase Bcl2 expression 14 days after gene transfer therapy (Fig. 7C). Furthermore, apoptosis 14 days after SCI was detected by TUNEL. Terminal deoxynucleotidyl transferase-mediated deoxyuridine triphosphate nick-end labeling-positive cells were

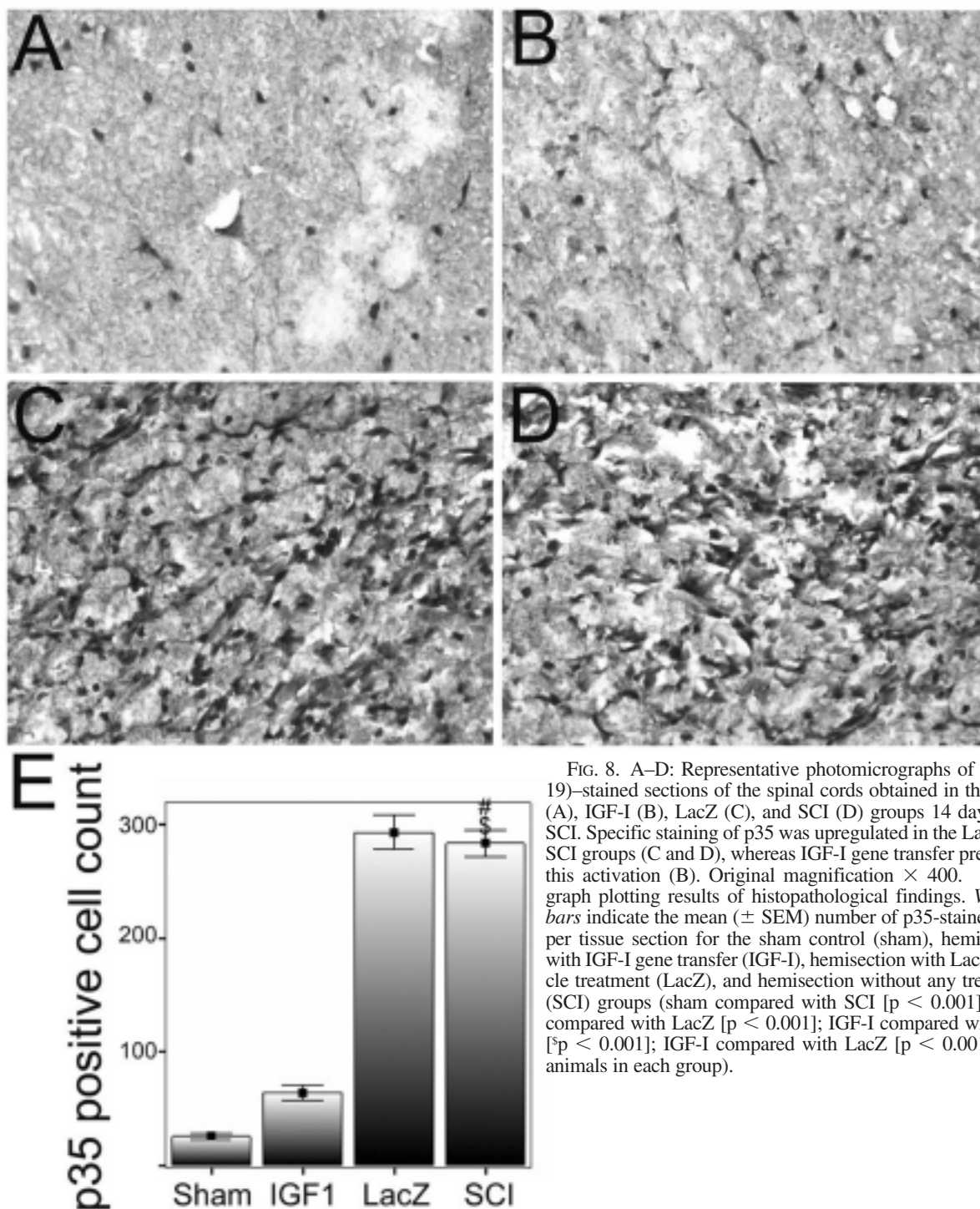


FIG. 8. A–D: Representative photomicrographs of p35(C-19)-stained sections of the spinal cords obtained in the sham (A), IGF-I (B), LacZ (C), and SCI (D) groups 14 days after SCI. Specific staining of p35 was upregulated in the LacZ and SCI groups (C and D), whereas IGF-I gene transfer prevented this activation (B). Original magnification  $\times 400$ . E: Bar graph plotting results of histopathological findings. Vertical bars indicate the mean ( $\pm$  SEM) number of p35-stained cells per tissue section for the sham control (sham), hemisection with IGF-I gene transfer (IGF-I), hemisection with LacZ vehicle treatment (LacZ), and hemisection without any treatment (SCI) groups (sham compared with SCI [ $p < 0.001$ ]; sham compared with LacZ [ $p < 0.001$ ]; IGF-I compared with SCI [ $p < 0.001$ ]; IGF-I compared with LacZ [ $p < 0.001$ ]; five animals in each group).

easily demonstrated in the pCMV–LacZ and SCI groups (Fig. 10C and D), whereas apoptosis was hardly detected in the pCMV–IGF-I group (Fig. 10B). Insulin-like growth factor–I gene transfer significantly attenuated apoptosis 14 days after SCI (Fig. 10F) (pCMV–IGF-I compared with pCMV–LacZ  $p < 0.001$ ; pCMV–IGF-I compared with SCI  $p < 0.001$ ). In our study we confirmed the antiapoptotic effect of IGF-I gene therapy with the inhibition of caspase-9 cleavage and the upregulation of Bcl2.

## Discussion

In the present study we have shown that a single intravenous IGF-I gene injection after spinal cord hemisection provides neuroprotective, antiinflammatory, and antiapoptotic effects in rats, and we hope that the findings of this study will open a new window for the treatment of SCI. We developed an *in vivo* gene transfection procedure in which a large volume of naked plasmid DNA solution is rapidly injected into the rat's tail vein.<sup>21,22</sup> One major con-



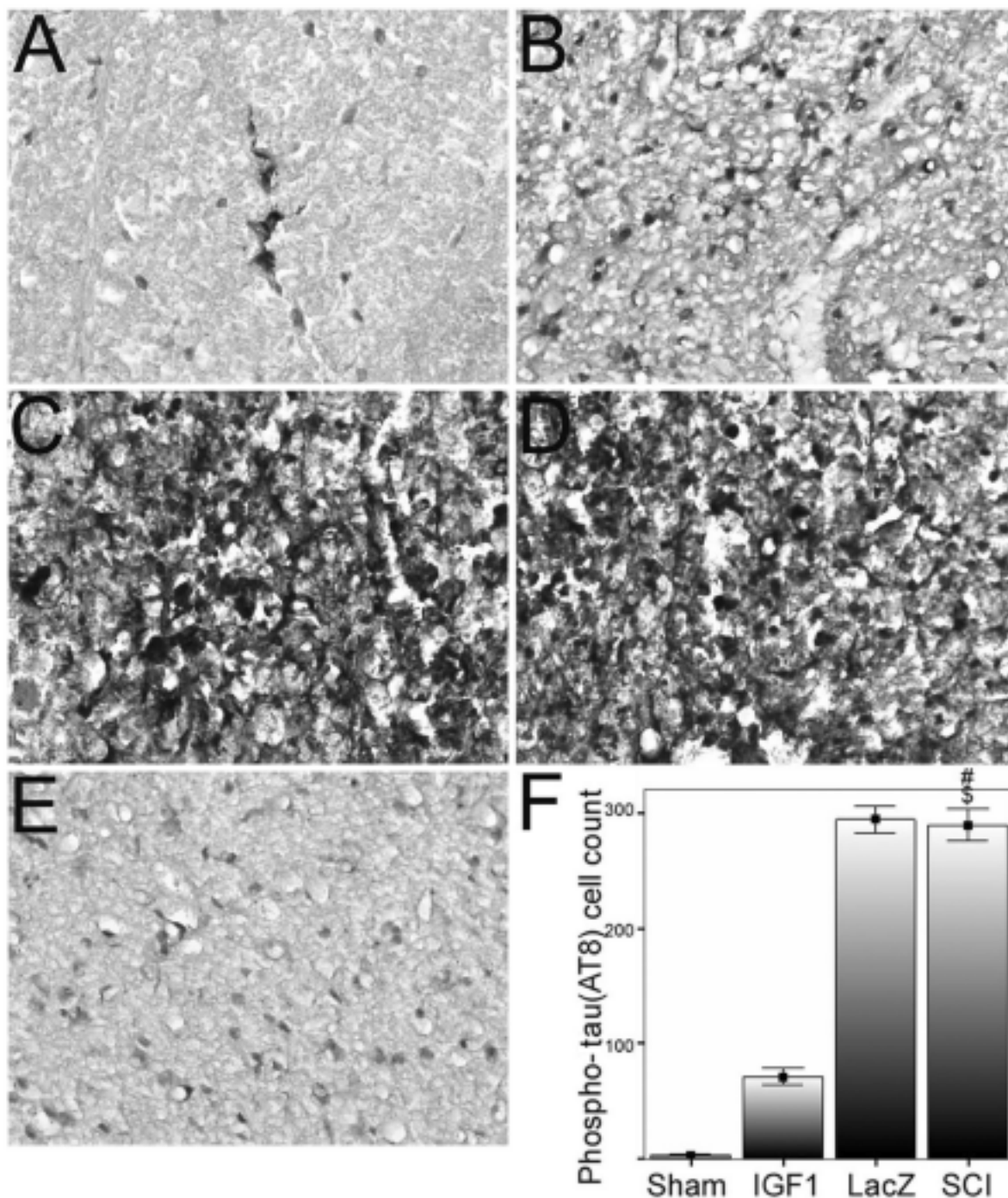


Fig. 9. A–E: Representative photomicrographs of phosphorylated tau (AT8)–stained sections of the spinal cords acquired in the sham controls (A), IGF-I group (B), LacZ group (C), SCI group (D), and negative control (omission of primary antibody) of LacZ group (E) 14 days after hemisection. Specific staining of AT8 was upregulated in the LacZ (C) and SCI (D) groups, whereas IGF-I gene transfer prevented this activation (B). Original magnification  $\times 400$ . F: Bar graph plotting results of histopathological findings. Vertical bars indicate the mean ( $\pm$  SEM) number of AT8-stained cells per tissue section for the sham controls (sham), hemisection with LacZ vehicle treatment (LacZ), and hemisection without any treatment (SCI) (sham compared with SCI [ $^*p < 0.001$ ]; sham compared with LacZ [ $p < 0.001$ ]; IGF-I compared with SCI [ $^*p < 0.001$ ]; IGF-I compared with LacZ [ $p < 0.001$ ]; five animals in each group).

cern regarding this gene transfer technique, however, is that it requires a fast injection of a large volume of solution, which may alter the physiological conditions of the

liver and heart. Indeed, after the injection, we noticed elevated levels of some liver enzymes, which eventually returned to baseline 3 to 10 days later.<sup>15</sup>

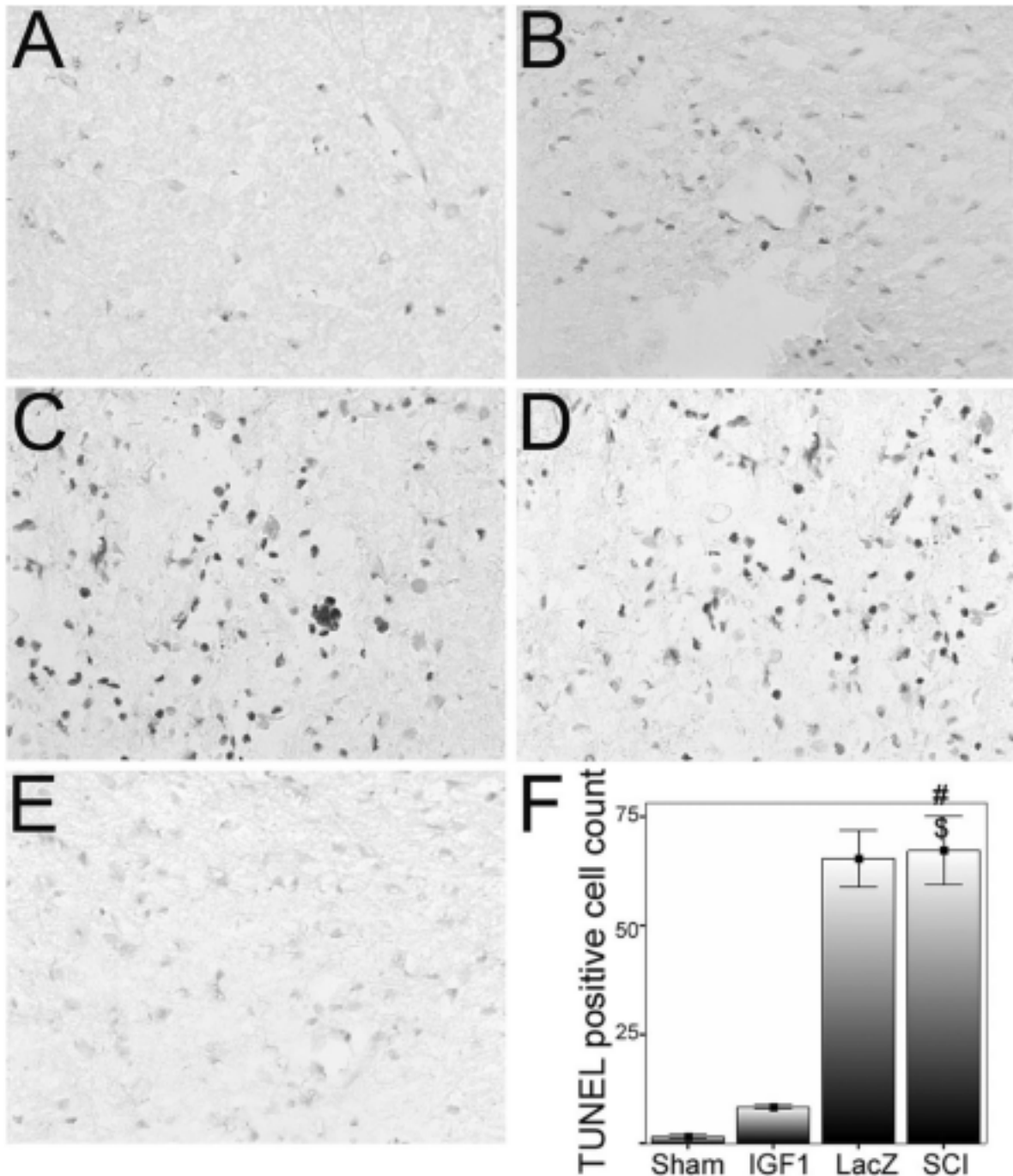


FIG. 10. Representative photomicrographs of TUNEL-stained sections of the spinal cords acquired in sham control (A), hemisection with IGF-I gene transfer (B), hemisection with LacZ vehicle treatment (C), hemisection without any treatment (D), and negative control (without Klenow enzyme) of hemisection with LacZ vehicle treatment (E) groups. Original magnification  $\times 400$ . F: Bar graph plotting results of histopathological findings. Vertical bars indicate the mean ( $\pm$  SEM) number of TUNEL-stained cells per tissue section for the sham controls (sham), hemisection with IGF-I gene transfer (IGF-I), hemisection with LacZ vehicle treatment (LacZ), and hemisection without any treatment (SCI) groups (sham compared with SCI [ $\#p < 0.001$ ]; sham compared with LacZ [ $p < 0.001$ ]; IGF-I compared with SCI [ $\$p < 0.001$ ]; IGF-I compared with LacZ [ $p < 0.001$ ]; five animals in each group).

We confirmed the presence of exogenous gene expression in both serum (Fig. 1) and the injured spinal cord (Fig. 2B1). Whetstone et al.<sup>23</sup> reported that SCI produces a biphasic opening of the blood–spinal cord barrier. The

first peak of abnormal leakage occurs within the first several hours after injury, whereas a second peak is evident between 3 and 7 days postinjury. We took advantage of this kind of time window to transflect IGF-I into the in-

## Insulin-like growth factor-I gene transfer in SCI

jured cord (Fig. 2B1). Additionally, significant elevation of serum IGF-I levels was shown for as many as 14 days after IGF-I gene transfer (Fig. 1). Within 14 days of injecting the IGF-I gene solution, there were relatively high levels of circulating IGF-I protein in the IGF-I-treated rats (Fig. 1). Furthermore, Pan and Kastin<sup>17</sup> showed that systemically administered IGF-I enters the central nervous system by a saturable transport system at the blood-brain barrier. This is one of the pharmacokinetic reasons why a single injection of the IGF-I plasmid can protect the spinal cord from SCI. The other direct immunohistochemical evidence of high-level IGF-I protein expression in injured spinal cord was present for as many as 14 days after gene transfer (Fig. 2B1).

In terms of motor function recovery, given that the primary injuries caused by the intentional SCI were equal in all three groups, we found no significant differences among pCMV-IGF-I, pCMV-LacZ, and SCI-alone groups 1 day after SCI (Fig. 3). The primary injury immediately causes cell death or necrosis at the injury site and then initiates a secondary injury process leading to an extension of the lesion into rostral and caudal areas of the spinal cord. Insulin-like growth factor-I gene transfer significantly improved the BBB Locomotor Scores 7 and 14 days after SCI (Fig. 3), partly because neuronal survival is preserved after hemisection (Fig. 4B and F). Moreover, within 14 days of the gene transfer therapy, there were relatively high levels of circulating IGF-I protein in the IGF-I-treated rats, and IGF-I is an anabolic growth factor for skeletal muscle that can stimulate myoblast proliferation and myofiber hypertrophy.<sup>18</sup> Another reason for near-total recovery after hemisection would be the adaptive plasticity of the motor pathways in the spinal cord hemisection model.<sup>7</sup>

The beneficial effects of IGF-I treatment were not solely restricted to neurons. We postulate that the size of a secondary neurodegeneration after SCI depends on the magnitude of the inflammatory events. In the immediate vicinity of the injury site, reactive astrocytes interweave to form a barrier, creating a glial scar, which can be an impediment to regenerating axons. Increased GFAP expression is a hallmark of reactive astrocytes, and this cytoskeletal protein contributes to a barrier effect of the glial scar for axonal extension. This response is fortified by the migration of microglia and macrophages to the damaged area. Astrocytes and microglia deserve special attention because of their roles in promoting the glial scar formation during and after the inflammatory process in spinal cord lesions.<sup>6,10</sup> Recently, Kaspar and colleagues<sup>12</sup> also obtained similar results in a mouse model of amyotrophic lateral sclerosis, suggesting a delayed activation of astrocytes in the IGF-I-treated animals. In our study we also demonstrated marked activation of astrocytes and microglia after SCI, with results shown by immunostaining of GFAP and CD11b, and IGF-I gene transfer effectively abolished these inflammatory responses (Fig. 5).

Regarding the downstream IGF-I expression, one molecule that may serve as a convergent point of different survival-promoting signaling pathways is Akt, a 60-kDa serine/threonine kinase that can be activated by IGF-I. The mechanism of IGF-I has been shown to increase the phosphorylated state of Akt, a protein kinase that is involved in blocking proapoptotic pathways through receptor-mediated

phosphatidylinositol 3-kinase signaling.<sup>20</sup> We found that IGF-I-treated animals had 100% higher levels of phosphorylated Akt than LacZ-treated controls (Fig. 6F). Phosphorylated Akt has been shown to prevent cleavage of caspase-9, thereby inhibiting apoptosis. Signaling within the apoptotic pathway, including the cleavage of caspase-3 and caspase-9, could be a target for SCI intervention. Insulin-like growth factor-I significantly reduced the amount of caspase-9 cleavage. At 14 days after SCI, IGF-I treatment had decreased the cleaved 37- and 39-kD subunits by more than 70% compared with LacZ treatment in the control group, indicating that IGF-I can block caspase activation involved in the apoptotic pathway (Fig. 7B). In addition, IGF-I-treated animals had 166% higher levels of Bcl2 than LacZ-treated controls (Fig. 7C). Furthermore, TUNEL staining was less evident in IGF-I-treated animals than in the LacZ group ( $8.4 \pm 1.14$  cells compared with  $65.4 \pm 14.84$  cells, respectively [five rats in each group],  $p < 0.001$ ) (Fig. 10). These findings provide molecular evidence of the antiapoptotic effect of IGF-I.

Another target of IGF-I signaling via Akt is GSK-3 $\beta$ . Insulin-like growth factor-I has been shown to stimulate the inhibitory serine phosphorylation of this pivotal enzyme in cultured neurons.<sup>9,13</sup> Insulin-like growth factor-I-induced inhibitory phosphorylation of GSK-3 $\beta$  at Ser9<sup>19</sup> relieves GSK-3 $\beta$ 's inhibition of glycogen synthase and the translation initiation factor eIF2B, thus promoting glycogen and protein synthesis. We found that IGF-I-treated rats had 30% higher levels of inhibitory GSK-3 $\beta$  at Ser9 than LacZ-treated controls (Fig. 7A). Tau, a microtubule-associated protein involved in neurofilament stabilization, is also a GSK-3 $\beta$  substrate. The authors of some studies have shown that IGF-I inhibits GSK-3 $\beta$  in neural cells and results in inhibition of tau hyperphosphorylation.<sup>8,22</sup> When it is hyperphosphorylated, tau is prone to form intracellular neurofibrillary tangles that contribute to neuronal degeneration. We have found that tau phosphorylation increased in the SCI and LacZ groups compared with the sham control group (Fig. 9), and IGF-I gene transfer could significantly inhibit tau hyperphosphorylation (Fig. 9B and F).

Recently we documented p35-p25-Cdk5 activation and tau hyperphosphorylation in rats that had undergone SCI.<sup>10</sup> Hyperphosphorylated tau is a major component of neurofibrillary tangles, one of the hallmarks of Alzheimer disease. It has been shown that Cdk5 is a kinase that phosphorylates the tau protein and that its endogenous activators, p35 and p25, regulate its activity.<sup>14</sup> We did not find significant change in the Cdk5 protein level after IGF-I gene transfer (Fig. 7D). On immunohistochemical evaluation, however, p35 was less stained in IGF-I-treated rats than LacZ-treated rats ( $63.8 \pm 14.11$  cells compared with  $293.0 \pm 33.20$  cells, respectively [five rats in each group],  $p < 0.001$ ) (Fig. 8E). It has been shown that p35 regulates not only the overall kinase activity of Cdk5 but also the sequential phosphorylation of Ser202 and Thr205 in tau.<sup>8</sup> Most of the tau studies have been focused on neurodegenerative Alzheimer disease, and our findings confirm the roles of p35 activation and tau hyperphosphorylation in SCI. Moreover, IGF-I gene transfer could inhibit this pathological cascade.

This study is the first step in confirming the potential effects of IGF-I gene transfer in SCI. Hemisection of the

spinal cord, however, is not the ideal model for preclinical study. Anderson et al.<sup>1</sup> have strongly recommended the use of contusion or compression injury models for pre-clinical validation according to consensus-based guidelines. Additionally, the follow-up duration of 2 weeks is short. A longer follow-up duration and the use of contusion or compression SCI models would be better in further study.

### Conclusions

In summary, intravenous administration of IGF-I after SCI activated Akt, abated GSK-3 $\beta$ , inhibited p35 activation, diminished tau hyperphosphorylation, ended microglia and astrocyte activation, inhibited neuron loss, and significantly improved neurological dysfunction. Furthermore, IGF-I attenuated caspase-9 cleavage, increased Bcl2, and thus inhibited apoptosis 14 days after SCI. These findings suggest that IGF-I gene transfer is a promising neuroprotective approach after SCI. Further studies involving alternative doses, routes, and vector paradigms are necessary to determine the potential clinical application of IGF-I in SCI.

### Disclaimer

The authors have no financial investment in any of the products mentioned in this manuscript.

### Acknowledgments

We thank Ms. Angel Sun and Yilu Lee for the sample collection and technical support.

### References

- Anderson DK, Beattie M, Blesch A, Bresnahan J, Bunge M, Dietrich D, et al: Recommended guidelines for studies of human subjects with spinal cord injury. **Spinal Cord** **43**:453–458, 2005
- Basso DM, Beattie MS, Bresnahan JC: A sensitive and reliable locomotor rating scale for open field testing in rats. **J Neurotrauma** **12**:1–21, 1995
- Bracken MB: Methylprednisolone and acute spinal cord injury: an update of the randomized evidence. **Spine** **26** (24 Suppl): S47–S54, 2001
- Cheng CM, Mervis RF, Niu SL, Salem N Jr, Witters LA, Tseng V, et al: Insulin-like growth factor-I is essential for normal dendritic growth. **J Neurosci Res** **73**:1–9, 2003
- Cheng CM, Reinhardt RR, Lee WH, Joncas G, Patel SC, Bondy CA: Insulin-like growth factor-I regulates developing brain glucose metabolism. **Proc Natl Acad Sci U S A** **97**:10236–10241, 2000
- Davies SJ, Field PM, Raisman G: Regeneration of cut adult axons fails even in the presence of continuous aligned glial pathways. **Exp Neurol** **142**:203–216, 1996
- Fujiki M, Kobayashi H, Inoue R, Ishii K: Immediate plasticity in the motor pathways after spinal cord hemisection: implications for transcranial magnetic motor-evoked potentials. **Exp Neurol** **187**:468–477, 2004
- Hashiguchi M, Saito T, Hisanaga S, Hashiguchi T: Truncation of CDK5 activator p35 induces intensive phosphorylation of Ser202/Thr205 of human tau. **J Biol Chem** **277**:44525–44530, 2002
- Hong M, Lee VM: Insulin and insulin-like growth factor-I regulate tau phosphorylation in cultured human neurons. **J Biol Chem** **272**:19547–19553, 1997
- Hung KS, Hwang SL, Liang CL, Chen YJ, Lee TH, Liu JK, et al: Calpain inhibitor inhibits p35-p25-cdk5 activation, decreases tau hyperphosphorylation, and improves neurological function after spinal cord hemisection in rats. **J Neuropathol Exp Neurol** **64**:15–26, 2005
- Hurlbert RJ: Strategies of medical intervention in the management of acute spinal cord injury. **Spine** **31** (11 Suppl):S16–S21, S36, 2006
- Kaspar BK, Llado J, Sherkat N, Rothstein JD, Gage FH: Retrograde viral delivery of IGF-1 prolongs survival in a mouse ALS model. **Science** **301**:839–842, 2003
- Lesort M, Johnson GV: Insulin-like growth factor-1 and insulin mediate transient site-selective increases in tau phosphorylation in primary cortical neurons. **Neuroscience** **99**:305–316, 2000
- Maccioni RB, Otth C, Concha II, Munoz JP: The protein kinase Cdk5. Structural aspects, roles in neurogenesis and involvement in Alzheimer's pathology. **Eur J Biochem** **268**:1518–1527, 2001
- Miao CH, Thompson AR, Loeb K, Ye X: Long-term and therapeutic-level hepatic gene expression of human factor IX after naked plasmid transfer in vivo. **Mol Ther** **3**:947–957, 2001
- Niblock MM, Brunso-Bechtold JK, Riddle DR: Insulin-like growth factor I stimulates dendritic growth in primary somatosensory cortex. **J Neurosci** **20**:4165–4176, 2000
- Pan W, Kastin A: Interactions of IGF-1 with the blood-brain barrier in vivo and in situ. **Neuroendocrinology** **72**:171–178, 2000
- Shansky J, Creswick B, Lee P, Wang X, Vandenberg H: Paracrine release of insulin-like growth factor-I from a bioengineered tissue stimulates skeletal muscle growth in vitro. **Tissue Eng** **12**:1833–1841, 2006
- Summers SA, Kao AW, Kohn AD, Backus GS, Roth RA, Pessin JE, et al: The role of glycogen synthase kinase 3 $\beta$  in insulin-stimulated glucose metabolism. **J Biol Chem** **274**:17934–17940, 1999
- Vincent AM, Feldman EL: Control of cell survival by IGF signaling pathways. **Growth Horm IGF Res** **12**:193–197, 2002
- Wang CH, Jawan B, Lee TH, Hung KS, Chou WY, Lu CN, et al: Single injection of naked plasmid encoding  $\beta$ -melanocyte-stimulating hormone protects against thioacetamide-induced acute liver failure in mice. **Biochem Biophys Res Commun** **322**:153–161, 2004
- Wang CH, Liang CL, Huang LT, Liu JK, Hung PH, Sun A, et al: Single intravenous injection of naked plasmid DNA encoding erythropoietin provides neuroprotection in hypoxia-ischemia rats. **Biochem Biophys Res Commun** **314**:1064–1071, 2004
- Whetstone WD, Hsu JY, Eisenberg M, Werb Z, Noble-Haeusslein LJ: Blood-spinal cord barrier after spinal cord injury: relation to revascularization and wound healing. **J Neurosci Res** **74**:227–239, 2003

Manuscript received January 5, 2006.

Accepted in final form September 15, 2006.

This work was supported by the National Science Council (Grant Nos. NSC 95-2314-B-182A-110, NSC 94-2314-B-182-032, and NSC 93-2314-B-182A-163), Department of Health (Grant No. DOH-TD-B-111-002), a Topnotch Stroke Research Center grant, and the Ministry of Education and Kaohsiung Chang Gung Memorial Hospital (Grant No. CMRPG 83058).

Address reprint requests to: Wen-Ta Chiu, M.D., Ph.D., Department of Neurosurgery, Taipei Medical University, Wan Fang Medical Center, 111 Section 3, Hsing-Long Road, Taipei 116, Taiwan. email: wtchiu@tmu.edu.tw.